Proceedings of the 28th IEEE
EMBS Annual International Conference
New York City, USA, Aug 30-Sept 3, 2006

Finite element analysis and experimental verification of multilayered tissue characterization using the thermal technique

Nachiket M. Kharalkar[1], Jonathan W. Valvano[1]
[1]Department of Electrical and Computer Engineering, The University of Texas at Austin, Texas, USA
E-mail: kharalkar@ieee.org

Abstract— **The objective of this research is to develop noninvasive techniques to determine thermal properties of layered biologic structures based on measurements from the surface. The self-heated thermistor technique is evaluated both numerically and experimentally. The finite element analyses, which confirm the experimental results, are used to study the temperature profiles occurring in the thermistor-tissue system.**

An *in vitro* tissue model was constructed by placing Teflon of varying thickness between the biologic tissue and the self-heated thermistor. The experiments were performed using two different-sized thermistors on six tissue samples. A self-heated thermistor was used to determine the thermal conductivity of tissue covered by a thin layer Teflon. The results from experimental data clearly indicate that this technique can penetrate below the thin layers of Teflon and thus is sensitive to the thermal properties of the underlying tissue. The factors which may introduce error in the experimental data are (i) poor thermal/physical contact between the thermistor probe and tissue sample, and (ii) water loss from tissue during the course of experimentation.

The finite element analysis was used to simulate the experimental conditions and to calculate transient temperature profile generated by the thermistor bead. The results of finite element analysis are in accordance with the experimental data.

Keywords—**Finite element method (FEM), thermal conductivity, self-heated thermistor**

I. INTRODUCTION

The ultimate goal of this paper is to perform thermal characterization using measurements taken at the surface of a two-layered tissue sample. In particular, if one knows the thickness and the thermal properties of the covering layer, then this technique can be used to measure thermal conductivity of the underlying tissue.

A. Significance

Many biologic tissues, such as skin, myocardium, kidney and vessels, have a structure where the surface is covered with a thin layer having properties fundamentally different than the underlying tissue. The knowledge of the thermal properties of the underlying tissue is extremely crucial in detection and treatment of certain medical disorders. This thermal scanning technique may have various applications, including but not limited to predicting the extent of injury due to skin burn, amount of damage due to frostbite, detection of tumors, and scanning of the coronary arteries.

The extent of injury due to skin burn is determined from the amount of alteration in the properties of underlying skin layers like epidermis and subcutaneous layer. For many years, researchers have tried to predict the degree of skin burn using different bioheat transfer models [1-3]. The analysis of the dorsal skin and in the subjacent skeletal muscle layer after CO_2 and Er^{3+} laser incisions using the light microscopic examinations has show an up to three times larger damage zone in the subcutaneous layer of skeletal muscle than in the connective tissue above [4]. The tumors normally have higher perfusion as compared to the healthy tissue [5]. Based on these differences, it may be possible to detect tumors below normal tissue and perhaps to differentiate amongst different types of tumors, possibly even malignant from benign [6]. The arterial wall is made up of different layers, having different thermal properties. This technique may help in penetrating below the endothelium and determining the composition of underlying layers [7].

B. Nomenclature

C = specific heat (J/kg-^{o}C)	Q = volumetric heat generation rate (mW/ cm^3)
ρ = density (kg/cm^3)	S = fibrous tissue sample
k = thermal conductivity (mW/cm-^{o}C)	L = Teflon layer
α = thermal diffusivity (cm^2/s)	τ = teflon thickness (cm)
r = radial distance in spherical coordinates (cm)	
T = temperature (^{o}C)	**Subscripts**
P = total thermistor electrical power (mW)	0 = initial
dT = volume average thermistor temperature rise (^{o}C)	∞ = final
t = time (s)	h = heated
F = fibrous tissue	F = fiber
	T = Teflon

C. Background

The self-heated thermistor technique for the measurement of tissue thermal properties has been in practice for a long time [8-11]. Valvano *et al.* have measured the thermal properties of biomaterials using the constant temperature and sinusoidal heating technique [12-13]. Valvano *et al.* have previously used the constant voltage heating technique for the measurement of thermal conductivity and diffusivity of arterial wall [14]. However

their work didn't include the penetration depth analysis and tissue characterization of multilayered tissues.

The finite element analysis is an effective tool to study the relationship between tissue thermal properties, thermistor power and the tissue-thermistor temperature profiles [15-16]. Hayes *et al.* have used finite element technique to validate the thermal conductivity measurements with a realistic thermistor geometry and electrical heating pattern [16]. Jain developed a thermal model having passive glass shell surrounding the active heated thermistor [17].

II. METHODOLOGY

The experiments were performed using two different sized glass encapsulated bead thermistors, BR32KA102K (radius = 0.041 cm, 1kΩ@25°C) and BR55KA102K (radius = 0.070 cm, 1kΩ@25°C) from Thermometrics. The constant voltage heating technique was used to heat the thermistors.

A. Self-heated thermistor technique

The thermistor was self-heated and the applied power P was continuously recorded along with the heated temperature response. The National Instruments data acquisition board PCI6110 was used to output the analog voltage and 16-bit PCI6013 board was used for acquiring the analog voltage at 10 kHz. A LabVIEW™ based data acquisition system was designed that outputs 0.149 V during the temperature sensing phase, which measured initial temperature, T_0. During the 20 second heating phase, 2.585 V was delivered to the thermistor, and the heated temperature, T_h, along with the applied power, P, were recorded. The temperature rise was the difference between the T_h and T_0.

$$dT = T_h - T_0 \tag{1}$$

The applied power P was nearly constant during the 20 second heating phase while the temperature rise dT varied considerably. Linear regression was used to separate transient (m) and the steady state (c) terms.

$$P / dT = m * t^{-1/2} + c \tag{2}$$

The following empirical equation was used to calculate the thermal conductivity [8-16].

$$k = \frac{1}{[\frac{a_1}{c} + a_2]} \tag{3}$$

Special thermistor probes were constructed for measurement of tissue thermal properties, by embedding the thermistors in the acrylic block in such a way that half of the spherical bead protruded from the acrylic block. This probe was placed on a two-layered tissue sample for the measurement of tissue thermal properties. A Hewlett-Packard 2804A quartz thermometer was used for the thermistor temperature calibration, while glycerol and 1% agar-gelled water were used as two liquids with known thermal properties to calculate coefficients a_1 and a_2 for each thermistor.

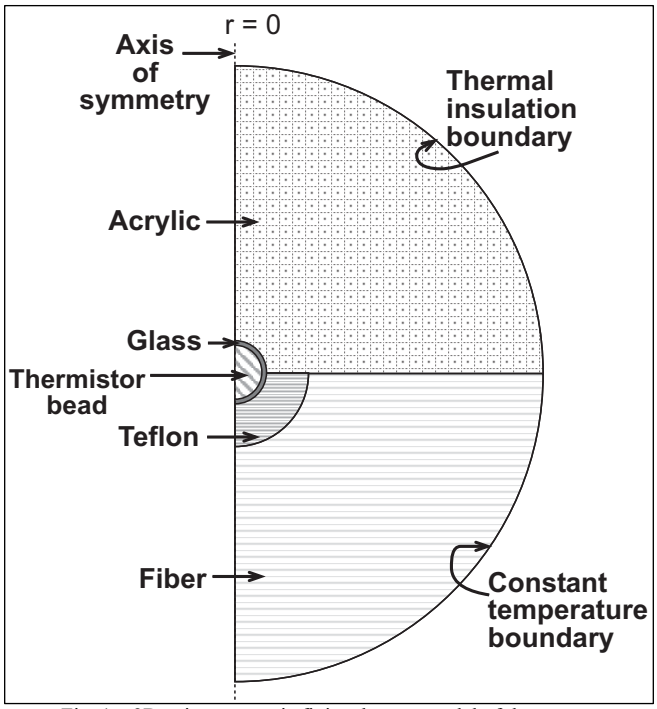

Fig. 1. 2D axis-symmetric finite element model of the system

B. Protocol

Samples of Angus beef consisting of mostly fibrous tissue were used for the experiments. The Teflon from DuPont was used as to simulate another layer of tissue with different thermal properties. The experiments were performed on 6 different tissue samples (S1 to S6). The tissue samples were placed on cotton gauze soaked in saline solution in order to prevent water loss from the tissue during the experiments. The measurements were done first on the bare tissue sample, then tissue covered by 1, 2, 4 and 8 layers of Teflon tape. In the end, measurements were again done on the bare tissue to record changes in the tissue thermal properties over time by the end of the experiments. Finally measurements were done on the 32 layers of Teflon tape without any tissue sample. The tissue-Teflon samples were kept in a closed chamber immersed in a temperature-controlled water bath, maintained at 37.5°C. The thermistor probe was placed on the samples and the measurements were taken only after the initial baseline temperature measured by the thermistor was stable. The thermistor was then heated for 20 seconds, during which P and dT were continuously recorded.

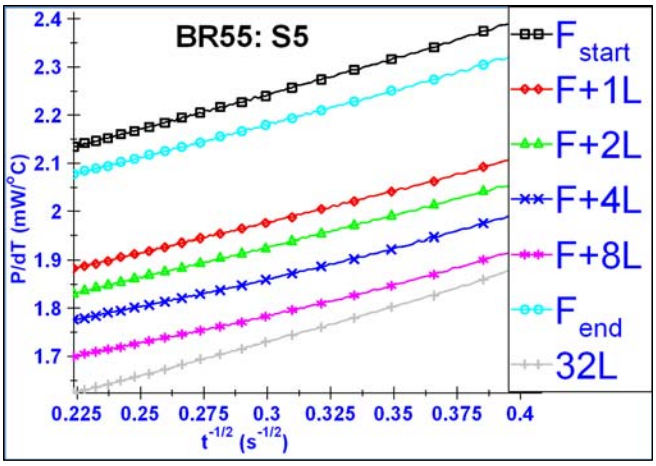

Fig. 2. Plot of P/dT versus $t^{-1/2}$ using BR55 on tissue sample S5

C. Finite element analysis

The finite element analysis was performed using COMSOL Multiphysics™ 3.2a. Equation 4 was used to model the system [18]. Equation 4 is the transient heat transfer equation. The 2D axi-symmetric model shown in figure 1 was used.

$$\rho C \frac{\partial T}{\partial t} + \nabla \cdot (-k \nabla T) = Q \qquad (4)$$

In equation 4, Q is the heat source term. Table I indicates the values of thermal properties of different materials modeled in figure 1. T_0 was assumed to be 37.5°C.

TABLE I
Thermal properties of different materials used in the FEA [18-22]

Material	k (mW/cm-°C)	C_p (J/kg-°C)	ρ (*10^{-6} kg/cm^3)
Acrylic sheet	1.9	1470	1190
Agar gel	6.0	4180	1000
Fiber	5.0	3700	1050
Glass	13.8	703	2203
Glycerol	2.9	2439	1260
Teflon tape	2.5	1172	2200
Thermistor bead	1.0	159	6300

III. RESULTS

A. Measured data

The tissue samples S1 to S3 were measured with the BR32 while S4 to S6 were measured with the BR55. The thickness of 1 layer of Teflon was 68*10^{-4} cm. P and dT was recorded during the 20 second heating phase and P/dT versus $t^{-1/2}$ plot was made for each experimental setup. A typical set of P/dT versus $t^{-1/2}$ data using BR55 on tissue sample S5 are shown in figure 2. The calibrated values of the thermal conductivity for all the experimental setups using both the thermistors have been summarized in table II. The measurements were performed on each tissue sample three times at the same position for different experimental conditions. The thermal conductivity value in table II for S1 to S6 is the average of three measurements.

TABLE II
Summary of thermal conductivity as obtained from experimental and simulated conditions

Exp. cond.	τ *10^{-4} (cm)	BR32 k (mW/cm-°C)				BR55 k (mW/cm-°C)			
		FEA	S1	S2	S3	FEA	S4	S5	S6
F_0	0	4.87	4.93	4.56	4.94	4.88	4.29	4.38	4.54
F+1L	68	4.34	4.00	3.57	3.12	4.53	3.95	3.49	3.31
F+2L	136	4.01	3.42	3.52	3.06	4.28	3.32	3.37	3.46
F+4L	272	3.63	3.17	3.32	2.82	3.91	3.16	3.21	3.20
F+8L	544	3.38	2.94	3.04	2.88	3.43	2.99	2.90	2.84
F_∞	0	-	4.58	4.61	4.62	-	4.09	4.21	4.31
32L	2176	2.58	2.39	2.47	2.21	2.56	2.58	2.53	2.37

B. Finite element analysis data

The applied power P from the experimental analysis was 3.25 mW. The volumetric heat generation rate Q in equation 4 for BR32 was 18000 mW/cm^3 and 3000 mW/cm^3 for BR55. Similar to the actual experiments simulations using the finite element modeling were done and the thermal conductivities for different experimental conditions were recorded. The summary of the simulated thermal conductivities is shown in table II along with the actual experimental readings. Figure 3 shows the comparison of temperature distribution in the thermistor-tissue system for BR32 on bare tissue and tissue covered by 8 layers of Teflon, at the end of heating phase (t = 20s).

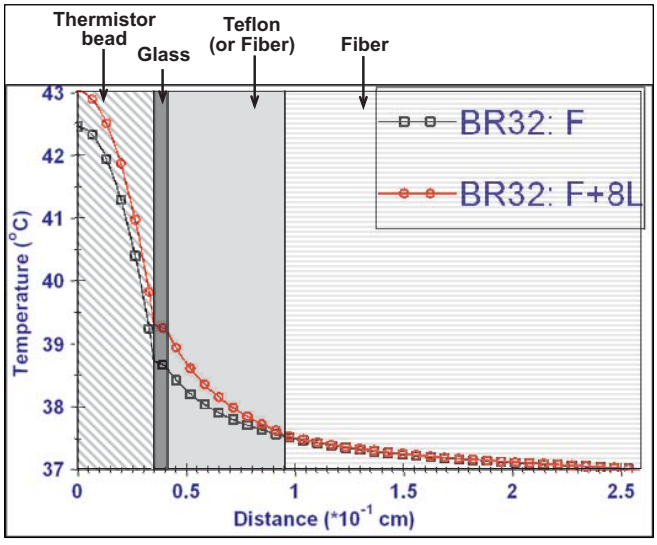

Fig. 3. Temperature profile of the thermistor-tissue system at t = 20s using BR32

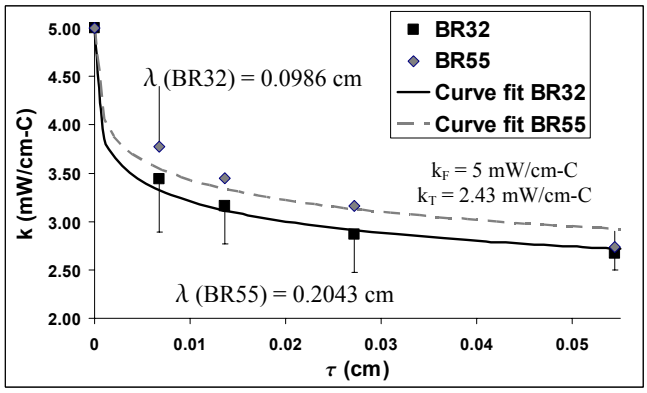

Fig. 4. Empirical fit of measured data

IV. DISCUSSION

The measured data was first normalized to the tissue conductivity (k_F) and Teflon thermal conductivity (k_T). The data, shown in figure 4, suggest that equation 5 can be used to determine underlying tissue conductivity if the thickness and thermal properties of the covering layer are known. Basically, the measured conductivity (k) is a function of both the outer Teflon layer (k_T) and the underlying tissue (k_F). In equation 5, λ is related to the thermistor size and was calculated using the least squared error technique.

$$\frac{1}{k} = \frac{1}{k_F} * e^{-\left(\frac{\tau}{\lambda}\right)^{1/3}} + \frac{1}{k_T} * \left[1 - e^{-\left(\frac{\tau}{\lambda}\right)^{1/3}}\right] \quad (5)$$

The thermal conductivity of the tissue at the end of the experiments (F_∞ in table II) was recorded 3 hours after data F_0 was recorded. The slight decrease in F_∞ as compared to F_0 may be due to the water loss from tissue during the course of experimentation. The finite element simulations show that the maximum temperature rise is at the center of the thermistor bead. The computer simulations indicate that the maximum temperature rise at the probe-tissue interface is about 2.25°C. The thermal conductivity readings from simulations are in close accordance with the experimental data.

V. CONCLUSION

The experimental data and the finite element simulations clearly indicate that this self-heated thermistor technique can penetrate and detect the presence of tissue hidden below another layer of tissue having different thermal properties. Conversely if the thermal properties of two tissue samples are known, this method could be further modified to give the thickness of the top layer. Proper thermal contact between thermistor probe and tissue sample is extremely important for this method to work successfully and is the main factor that may introduce errors in the experiment. The computer simulations indicate that the temperature rise within the tissue is extremely small and may not cause significant damage to the tissue due to heating.

ACKNOWLEDGMENT

Authors would like to thank National Instruments™ for generously providing all their softwares for free.

REFERENCES

[1] Diller, K. R. and Hayes, L. J., "Analysis of tissue injury by burning: Comparison of *in situ* and skin flap models," *Int. J. Heat Mass Transfer*, vol. 34, pp. 1393–1406, 1991.
[2] Liu, J., Chen, X., and Xu, L., "New Thermal Wave Aspects on Burn Evaluation of Skin Subjected to Instantaneous Heating", *IEEE Trans. Biomed. Eng.*, vol. 46, no. 4, pp. 420-428, 1999.
[3] Torvi, D. A., Dale, J. D., "A finite element model of skin subjected to a flash fire", J Biomech Eng., 116(3):250-5, 1994
[4] Frenz, M., Mischler, Ch., Romano, V., Forrer, M., Müller, O. M., and Weber, H. P., "Effect of mechanical tissue properties on thermal damage in skin after IR-laser ablation", *Applied Physics B: Lasers and Optics*, vol. 52, Number 4; pp: 251 – 258; 1991.
[5] Song, C. W., "Blood flow in tumors and normal tissues in hyperthermia", Hyperthermia in cancer therapy, Boston: G.K. Hall Medical Publishers, pp. 187–206, 1983.
[6] Cheng, H. M. and Plewes, D. B., "Tissue Thermal Conductivity by Magnetic Resonance Thermometry and Focused Ultrasound Heating", J. of Mag. Res. Ima., 16:598–609, 2002.
[7] Bhatia V, Bhatia R, Dhindsa S, Virk A, "Vulnerable Plaques, Inflammation and Newer Imaging Modalities", J. Postgrad. Med., 49:361-8, 2003.
[8] Patel, P. A., Valvano, J. W., Pearce, J. A., Prahl, S. A., and Denham, C. R., "A Self-Heated Thermistor Technique to Measure Effective Thermal Properties from the Tissue Surface", Journal of Biomech. Eng., Vol. 109, pp. 330-335, 1987.
[9] Balasubramaniam, T.A., Bowman, H.F., "Thermal Conductivity and Thermal Diffusivity of Biomaterials: A Simultaneous Measurement Technique", J. of Biomech. Eng., Vol. 99, pp. 148-154, 1977.
[10] Holmes, K.R., Chen, M.M., "In vivo Tissue Thermal Conductivity and Local Blood Perfusion Measured with Heat Pulse-decay Method", Advances in Bioeng., pp. 113-115, 1980.
[11] Valvano, J.W., et al., "The Simultaneous Measurement of Thermal Conductivity, Thermal Diffusivity and Perfusion in Small Volume of Tissue". J. of Biomech. Eng., Vol. 106, pp. 192-197, 1984.
[12] Valvano, J. W., Cochran, J. R. and Diller, K. R., "Thermal conductivity and diffusivity of biomaterials with self-heated thermistors", Inter. J. of Thermophysics, vol. 6, no. 3, pp. 301-311, 1985.
[13] Valvano, J.W., Nho, S., "Tissue Thermal Diffusivity Measured with Sinusoidal Heated Thermistors," *ASME Winter Annual Mtg., Atlanta, HTD* Vol. 179, pp. 9-14, 1991.
[14] Valvano, J. W. and Chitsabesan, B., "Thermal conductivity and diffusivity of arterial wall and atherosclerotic plaque", *Lasers in the life sci.* 1(3), pp. 231-236, 1987.
[15] Patel, P., Valvano, J. W. and Hayes. L., "A finite element analysis of a surface thermal probe", *Thermo., heat, and mass trans. in biotech.,* ASME winter annual meeting, 1987.
[16] Valvano, J. W. and Hayes. L, "Steady-state analysis of self-heated thermistors using finite elements", *J. of biomech. Eng.*, vol. 107, pp. 77-80, 1985.
[17] Jain, R. K., *J. of biomech. Eng.* 101:82, 1979.
[18] COMSOL Multiphysics™, version 3.2a, User's guide
[19] http://www.hukseflux.com/thermal%20conductivity/thermal.htm
[20] http://hypertextbook.com/physics/thermal/heat-sensible/
[21] http://www.reade.com/Products/Oxides/copper_oxide.html
[22] Acrylite FF data sheet, www.cyro.com